Antiviral Research 94 (2012) 232–241

Contents lists available at SciVerse ScienceDirect

Antiviral Research

journal homepage: www.elsevier.com/locate/antiviral

Profile of stress and toxicity gene expression in human hepatic cells treated with Efavirenz

Leysa J. Gomez-Sucerquia [a,c], Ana Blas-Garcia [a,b], Miguel Marti-Cabrera [a,b], Juan V. Esplugues [a,b,c], Nadezda Apostolova [a,b,*]

[a] Departamento de Farmacología, Facultad de Medicina, Universitat de València, Valencia, Spain
[b] Centro de Investigación Biomédica en Red: Área temática de Enfermedades hepáticas y digestivas (CIBERehd), Valencia, Spain
[c] Fundación para la Investigación Hospital Universitario Dr. Peset, Valencia, Spain

ARTICLE INFO

Article history:
Received 18 January 2012
Revised 5 April 2012
Accepted 10 April 2012
Available online 24 April 2012

Keywords:
Mitochondria
Hepatotoxicity
HIV
NNRTI
Differential gene expression
Stress response

ABSTRACT

Hepatic toxicity and metabolic disorders are major adverse effects elicited during the pharmacological treatment of the human immunodeficiency virus (HIV) infection. Efavirenz (EFV), the most widely used non-nucleoside reverse transcriptase inhibitor (NNRTI), has been associated with these events, with recent studies implicating it in stress responses involving mitochondrial dysfunction and oxidative stress in human hepatic cells. To expand these findings, we analyzed the influence of EFV on the expression profile of selected stress and toxicity genes in these cells.

Significant up-regulation was observed with Cytochrome P450, family 1, subfamily A, polypeptide 1 (*CYP1A1*), which indicated metabolic stress. Several genes directly related to oxidative stress and damage exhibited increased expression, including Methalothionein 2A (*MT2A*), Heat shock 70 kDa protein 6 (*HSPA6*), Growth differentiation factor 15 (*GDF15*) and DNA-damage-inducible transcript 3 (DDIT3). In addition, Early growth response protein 1 (*EGR1*) was enhanced, whereas mRNA levels of the inflammatory genes Chemokine (C-X-C motif) ligand 10 (*CXCL10*) and Serpin peptidase inhibitor (nexin, plasminogen activator inhibitor type 1), member 1 (*SERPINE1*) decreased and increased, respectively. This profile of gene expression supports previous data demonstrating altered mitochondrial function and presence of oxidative stress/damage in EFV-treated hepatic cells, and may be of relevance in the search for molecular targets with therapeutic potential to be employed in the prevention, diagnosis and treatment of the hepatic toxicity associated with HIV therapy.

1. Introduction

Combined Antiretroviral Therapy (cART) has rendered human acquired immunodeficiency syndrome (AIDS) a chronic rather than mortal illness in the developed world. However, as the disease has come under control, there has been increasing concern about the adverse effects of this medication. Metabolic disturbances, particularly those related to lipid homeostasis, appear in nearly half of cART patients (Caron-Debarle et al., 2010) whereas significant drug-induced hepatotoxicity has been identified in up to a quarter of patients, a figure that probably belies actual rates, as 50% of subjects with increased liver enzymes are asymptomatic (Inductivo-Yu and Bonacini, 2008; Núñez, 2006, 2010). Mitochondrial toxicity is one of the main mechanisms responsible for cART-induced side effects. It has been attributed primarily to one component of this multi-drug therapy, namely nucleoside analogue reverse transcriptase inhibitors (NRTI), which are capable of inhibiting the enzyme responsible for mtDNA replication, mitochondrial DNA polymerase gamma (Pol-γ) (Walker et al., 2002). cART regimens usually comprise two NRTI plus either a boosted protease inhibitor (PI) or a non-nucleoside reverse transcriptase inhibitor (NNRTI) (AIDSinfo, 2011). Efavirenz (EFV) is the most widely prescribed NNRTI. It is largely considered a safe drug, however its use has been related to psychiatric symptoms and to a lesser extent lipid and metabolic disorders and hepatotoxicity (Tashima et al., 2003; Gutierrez et al., 2005; Manfredi et al., 2005; Maggiolo, 2009). The mechanisms responsible for these toxic effects remain largely unknown; however, despite the fact that EFV does not inhibit Pol-γ, some of

Abbreviations: EFV, Efavirenz; HAART, highly active antiretroviral therapy; NRTI, nucleoside reverse transcriptase inhibitor; NNRTI, non-nucleoside reverse transcriptase inhibitor; ROS, reactive oxygen species; $\Delta\Psi_m$, mitochondrial transmembrane potential; DNA, polymerase gamma (Pol-γ); ER, endoplasmatic reticulum; UPR, unfolded protein response.

* Corresponding author at: Departamento de Farmacología, Facultad de Medicina, Universidad de València, Avda. Blasco Ibáñez n. 15-17, 46010 Valencia, Spain. Tel.: +34 963864630; fax: +34 963983879.
E-mail address: nadezda.apostolova@uv.es (N. Apostolova).

0166-3542/$ - see front matter © 2012 Elsevier B.V. All rights reserved.
http://dx.doi.org/10.1016/j.antiviral.2012.04.003

its actions display features of mitochondrial dysfunction. Recent studies report deleterious effects by EFV in human hepatic cells that point to specific mitochondrial alterations and metabolic disturbances (Apostolova et al., 2010; Blas-García et al., 2010). In particular, the stress response observed included major bioenergetic changes manifested as a reduction in mitochondrial oxygen consumption with specific inhibition at Complex I of the electron transport chain, a decrease in ATP production, a drop in the mitochondrial membrane potential ($\Delta\Psi_m$) and an augmentation in reactive oxygen species (ROS) generation. An enhancement of mitochondrial mass was also detected and associated with the induction of autophagy (in particular, mitophagy) and apoptosis (Apostolova et al., 2010, 2011). Importantly, the highest concentration of EFV employed in these studies (50 μM) compromised the viability and proliferation of Hep3B cells, leading to cell cycle arrest and induction of apoptotic cell death (Apostolova et al., 2010). In order to provide an initial assessment of potential stress-related pathways involved in the toxic effects of EFV, in the present work we have studied the expression of specific stress and toxicity-responsive genes in human hepatoma cells (Hep3B) treated with the same, clinically relevant, concentrations of the compound previously shown to modify mitochondrial function without exerting a major effect on cellular viability (10 and 25 μM). Several validating experiments have also been performed in primary human hepatocytes.

2. Materials and methods

2.1. Reagents and drugs

Efavirenz acquired from Sequoia Research Products (Pangbourne, UK), was dissolved in methanol (3 mg/ml) and the purity (98–100%) and stability of the solutions were evaluated by HPLC. The EFV concentrations employed (10 and 25 μM) are clinically relevant and were chosen taking into account the important inter-individual variability reported for the pharmacokinetics of this drug (Burger et al., 2006).

2.2. Cell culture

Hep3B cells (ATCC HB-8064) were employed due to their metabolic competence, as they possess an active cytochrome P450 system despite constituting a transformed human hepatoma cell line (Zhu et al., 2007). Specifically, EFV is primarily metabolized by CYP2B6, the activity of which has been reported to in Hep3B cells (Lin et al., 2012). These cells were cultured in MEM supplemented with 1 mM non-essential amino acids, 10% heat-inactivated foetal bovine serum, penicillin (50 units/mL) and streptomycin (50 μg/mL). Unless stated otherwise, all the reagents employed were purchased from GIBCO (Invitrogen, Eugene, OR). Primary human hepatocytes were obtained from liver biopsies (one man, two women), isolated following a two-step collagenase protocol and cultured as described elsewhere (Apostolova et al., 2010). The protocols employed complied with European Community guidelines for the use of human experimental models and were approved by the Ethics Committee of the University of Valencia, Valencia. Cell cultures were maintained in an incubator (IGO 150, Jouan, Saint-Herblain Cedes, France) at 37 °C in a humidified atmosphere of 5% CO2/95% air (AirLiquide Medicinal, Valencia, Spain). Treatments of Hep3B cells were performed in subconfluent *t*-25 flask cell cultures (1.5×10^6 cells/flask seeded one day before the experiment), whereas primary hepatocytes were cultured and treated in collagen- precoated multi-well plates, "BioCoat" (BD, Madrid, Spain). In vivo, EFV has been shown to have high plasma protein binding. This fact was taken into account and thus 10% serum was present during the entire period of exposure to the drug.

2.3. RT^{2}Profiler™ PCR array

Expression of 84 genes was studied by real time PCR-Array (RT^{2}Profiler™ PCR Array: Human Stress and Toxicity Finder™, SABiosciences, Frederick, MD, Ref. PAHS-003C) using 5 housekeeping genes. For these experiments, Hep3B cells were treated with EFV for 8 h (25 μM, $n = 3$) or 24 h (10 and 25 μM, $n = 2$).

2.3.1. RNA isolation

Total RNA was extracted with the RNeasy Mini Kit (Qiagen, Hilden, Germany) following the manufacturer's instructions and eluted in 30 μl of water. It was then quantified using a NanoDrop® ND-1000 spectrophotometer (NanoDrop Technologies, Wilmington, DE).

2.3.2. First-strand cDNA synthesis

First strand cDNA synthesis was achieved using the RT^2 First Strand Kit (SABiosciences, Frederick, MD). One microgram of total RNA was reverse transcribed in a final volume of 20 μl following the manufacturer's instructions and including a genomic DNA elimination step. Reverse transcriptase was inactivated by heating at 95 °C for 5 min. cDNA was diluted to 111 μl by adding RNase-free water and was stored at −20 °C until use.

2.3.3. PCR array

cDNA was mixed with RT^2 SYBR green/ROX qPCR master mix (SABiosciences, Frederick, MD) following the manufacturer's instructions. Thereafter, 25 μl/well were loaded in 96 well plates with pre-dispensed specific primer sets of the RT2 Profiler PCR Array (SABiosciences, catalog number PAHS-003C). PCR array experiments (10 min at 95 °C followed by 40 cycles of 15 s at 95 °C and 1 min at 60 °C) were performed using an ABI 7900HT FAST instrument (Applied Biosystems, Foster City, CA).

2.3.4. Data analysis

We employed the ΔΔCt method using the online analysis tool provided by the supplier of the PCR arrays (http://www.sabiosciences.com/pcrarraydataanalysis.php). Genes with Ct values greater than 35 cycles were considered non-detectable. An average of five house-keeping genes [beta-2-microglobulin (*B2M*), hypoxanthine phosphoribosyltransferase 1 (*HPRT1*), ribosomal protein L12a (*RPL13A*), glyceraldehyde-3-phosphate dehydrogenase (*GAPDH*), and beta-actin (*ACTB*)] was used to obtain the ΔCt value for each gene of interest. The ΔΔCt value was calculated according to the difference between the ΔCt of the treatment group and that of the control group. The fold-change was calculated by 2^(−ΔΔCt), which represents the level of the expression of each gene in the EFV-treated sample vs that in the vehicle control sample.

2.4. RT-PCR validation

The array was validated by performing real time RT-PCR (at least 3 times in duplicate) using mRNA of Hep3B cells treated with the vehicle or EFV (10 and 25 μM at 8 and 24 h) and primary human hepatocytes treated with vehicle or EFV (10 and 25 μM at 24 h). Six representative genes of the array were selected according to their level of expression, and RT-PCRs were performed with the same sets of primers used in the gene array (SABiosciences, Frederick, MD).

2.4.1. RNA isolation and First-strand cDNA synthesis

RNA was isolated and cDNA synthesis was performed as described above, using the same reagents and protocols as in the gene array study.

2.4.2. Real Time PCR

PCR reactions were performed in a Carousel-based LightCycler® 2.0 Real Time PCR System (Roche Applied Biosystems) using 9 ng of cDNA mixed with LightCycler® FastStart DNA MasterPLUS SYBR Green I master mix (Roche Applied Science, Mannheim, Germany) following the instructions in the manual. Primers (1 μM) were added in a final reaction volume of 10μL. For amplification, reactions were performed as follows: 5 min denaturalization at 95 °C, followed by 35 cycles under conditions shown in Table 1 and 10 min of denaturalization. Human cyclophilin A (*CyPA*) was employed as a housekeeping gene, and reactions were performed as follows: 5 min denaturalization at 95 °C, followed by 35 cycles of 1 s at 95 °C, 5 s at 58 °C and 17 s at 72 °C. The primers used were *CyPA*(s) 5′CGTCTCCTTTGAGCTGTTTG-3′ (sense) and *CyPA*(as) 5'TCTGGTCGTTCTTCTAGTGG-3′ (antisense). The relative expression of *CyPA* was also confirmed with a second house-keeping gene, *ACTB* (β- actin) using the following primers: (s) 5'GGACTTC GAGCAAGAGATGG 3′ and (as), 5′AGCACTGTGTTGGCGTACAG 3′ (TIB MOLBIOL, Berlin, Germany).

To quantify the amounts of the template, a standard curve for each analyzed gene was prepared with serial dilutions of total RNA and was included in each run. The specificity of the amplified products was verified by melting curve analysis. To normalize the results, interpolated values for each sample were divided by the corresponding values for the housekeeping gene, and results were expressed as the fold induction of the specific gen/*CyPA* ratio for each treatment vs the corresponding control group.

Gene symbol	Catalog number	RefSeq accession #	Reference position	Band size (bp)	Annealing temperature (°C)
ATM	PPH00325B	NM_000051.3	10865	161	55
CXCL10	PPH00765E	NM_001565.2	765	111	55
MT2A	PPH01518B	NM_005953.3	352	83	55
HSPA6	PPH01192E	NM_002155.3	2552	167	57
SERPINE1	PPH00215E	NM_000602.2	2658	96	55
EGR1	PPH00139A	NM_001964.2	1049	178	55

2.5. Western blot

Whole-cell protein extracts were obtained using *t*-25 flask cell cultures of Hep3B cells and 6-well plates with primary human hepatocytes, by lysing cell pellets in 50–100 μL complete lysis buffer (20 mM HEPES pH = 7.4, 400 mM NaCl, 20% (v/v) glycerol, 0.1 mM EDTA, 10 μM Na_2MoO_4, 1 mM DTT) supplemented with protease inhibitors (“Complete Mini” protease inhibitor cocktail, and “Pefabloc”, both from Roche Diagnostics), and phosphatase inhibitors mixture: 10 μM NaF, 10 mM $NaVO_3$, 10 mM p-nitrophenylphosphate (PNPP) and 10 mM β-glycerolphosphate. Samples were vortexed, incubated on ice for 15 min, vortexed again and centrifuged in a microcentrifuge at 16100*g* for 15 min at 4 °C. Protein content was quantified employing the “BCA Protein Assay Kit” (Pierce, Thermo Scientific, Rockford, IL). SDS-PAGE and WB were performed using standard methods (BioRad, Hercules, CA), with 50 μg of the protein extract and employing primary antibodies: anti-HSPA6 rabbit polyclonal, anti-MT2A mouse monoclonal and anti-actin rabbit polyclonal antibody (all three from Sigma-Aldrich, Steinheim, Germany), at 1:1000, and a secondary antibody, peroxidase-labeled anti-rabbit IgG (Vector laboratories, Burlingame, CA) at 1:5000 or anti-mouse antibody (Dako Glostrup, Denmark) at 1:2000. Immunolabeling was detected using the enhanced chemiluminescent reagent ECL (Amersham, GE Healthcare, Little Chalfont, UK) or SuperSignal WestFemto (Pierce, Thermo Scientific, Rockford, IL), and was visualized with a digital luminescent image analyzer (FUJIFILM LAS 3000, Fujifilm). ImageQuant software v. 4.0. was used for densitometric analysis.

2.6. Statistical analysis

All values are mean ± S.E.M. Data were analyzed using GraphPad Prism v.3. software with “Student’s t-test” and statistical significance was assessed in EFV vs vehicle ($^{*}p < 0.05$, $^{**}p < 0.01$ and $^{***}p < 0.001$).

3. Results

We have studied the expression of 8 groups of genes involved in metabolic stress; oxidative stress; heat shock; proliferation and carcinogenesis; growth arrest and senescence; inflammation; necrosis/apoptosis (DNA damage and repair) and apoptosis signalling. The metabolism of EFV is largely cytochrome P450-mediated; therefore, the fact that incubation of Hep3B cells with 25 μM EFV for only 8 h significantly modified the expression of several genes involved in drug metabolism is relevant (Table 1 and Fig. 1). In particular, there was up-regulation of *CYP1A1* and down-regulation of *CYP2E1* and *CYP7A1*. In addition, we observed a reduction in the expression of cytochrome p450 oxidoreductase (*POR*), Glutathione S-transferase M3 (*GSTM3*) and Flavin-containing monooxygenases-1 (*FMO1*) and -5 (*FMO5*). Of the various oxidative stress-responsive genes analyzed, the mitochondrial form of superoxide dismutase (*SOD2*) and, to an even greater extent, metallothionein 2A (*MT2A*) were found to have increased, whereas there was a reduction in the expression of Catalase (*CAT*) and Prostaglandin- endoperoxide synthase 1 (*PTGS1*). No significant changes were detected in the expression of Alpha-crystallin B chain (*CRYAB*), Glutathione peroxidase 1 (*GPX1*), Glutathione reductase (*GSR*), Peroxiredoxin-1 and -2 (*PRDX1* and *2*), or Superoxide dismutase 1 (*SOD1*). Among the various heat shock-related proteins evaluated, including two *DNAJ* genes, several *HSPA* and *HSP90*, *HSPB*, *HSPD*, *HDPE*, *HSPH*, and *HSF1*, only the expression of *HSPA2* (down-regulation) and *HSPA6* (up-regulation) was found to be altered. In terms of genes implicated in proliferation and/or carcinogenesis, Cyclin ND1 (*CCND1*) and Early growth response 1 (*EGR1*) were up-regulated, Cyclin G1 (*CCNG1*) and Proliferating cell nuclear antigen (*PCNA*) exhibited decreased mRNA levels, and no significant modifications were observed in the expression of Cyclin C (*CCNC*) or E2F transcription factor 1 (*E2F1*). Of the genes associated with growth arrest and senescence, a major increase was observed in Growth differentiation factor 15 (*GDF15*), while Cyclin-dependent kinase inhibitor 1A (*CDKN1A*) and Mdm2 p53 binding protein homolog (*MDM2*) displayed a minor but statistically significant increase. No changes were detected in the expression of DNA-damage-inducible transcript 3 (*DDIT3*), Growth arrest and DNA-damage-inducible alpha (*GADD45A*), Insulin-like growth factor binding protein 6 (IGFBP6) or Tumor protein p53 (*TP53*). Of the genes implicated in inflammation, a significant up-regulation was detected with Serpin pepti-

Table 1
RT^2 Human Stress and Toxicity Pathway Finder™ PCR expression array analysis was performed after treatment of Hep3B cells with 10 μM EFV for 8 h ($n = 3$) and with 10 μM and 25 μM EFV for 24 h ($n = 2$). Numerical gene expression changes induced by EFV treatment were compared to those after exposure to the vehicle (0.25% methanol). Data are represented as fold change and mean ± SEM, and were analyzed by a Student's *t*-test, $^{*}p < 0.05$, $^{**}p < 0.01$, $^{***}p < 0.001$ vs vehicle.

			Fold change gene expression vs vehicle					
		Description	8 h		24 h			
Refseq	Symbol	Metabolic stress	10 (μM EFV)	*p* value	10 (μM EFV)	*p* value	25 (μM EFV)	*p* value
NM_000499	*CYP1A1*	Cytochrome P450, family 1, subfamily A, polypeptide 1	3.16	**0.0148**	1.84	**0.0035**	3.43	**0.0013**
NM_000773	*CYP2E1*	Cytochrome P450, family 2, subfamily E, polypeptide 1	0.44	**0.0001**	0.69	0.1956	0.64	0.5116
NM_000780	*CYP7A1*	Cytochrome P450, family 7, subfamily A, polypeptide 1	0.17	**0.038**	0.90	0.7934	0.90	0.8938
NM_001979	*EPHX2*	Epoxide hydrolase 2, cytoplasmic	1.05	0.7262	0.93	0.2808	1.85	0.0784
NM_002021	*FMO1*	Flavin containing monooxygenase 1	0.24	**0.0066**	0.44	0.3758	0.37	**0.0262**
NM_001461	*FMO5*	Flavin containing monooxygenase 5	0.57	0.0899	1.02	0.889	1.14	0.3059
NM_000849	*GSTM3*	Glutathione S-transferase mu 3 (brain)	0.61	**0.0002**	1.01	0.9614	0.77	0.7474
NM_000941	*POR*	P450 (cytochrome) oxidoreductase	0.65	**0.0056**	0.99	0.954	1.54	0.4301
Refseq	Symbol	Oxidative Stress						
NM_001752	*CAT*	Catalase	0.57	0.0987	0.97	0.7298	1.28	0.3865
NM_001885	*CRYAB*	Crystallin, alpha B	0.86	0.5965	0.89	0.7882	0.56	0.0701
NM_000581	*GPX1*	Glutathione peroxidase 1	0.78	0.2295	1.23	0.4879	1.52	0.071
NM_000637	*GSR*	Glutathione reductase	1.08	0.8389	1.13	0.1478	1.36	0.6981
NM_002133	*HMOX1*	Heme oxygenase (decycling) 1	1.00	0.9954	1.03	0.9152	1.17	0.7362
NM_005953	*MT2A*	Metallothionein 2A	2.32	**0.0033**	1.99	**0.0103**	3.59	0.0546
NM_002574	*PRDX1*	Peroxiredoxin 1	0.96	0.7409	1.58	0.3984	1.69	**0.0073**
NM_005809	*PRDX2*	Peroxiredoxin 2	0.64	0.3295	1.12	0.1278	1.33	0.3881
NM_000962	*PTGS1*	Prostaglandin-endoperoxide synthase 1 (prostaglandin G/H synthase and cyclooxygenase)	0.65	**0.0063**	1.32	0.7088	0.76	**0.0493**
NM_000454	*SOD1*	Superoxide dismutase 1, soluble	0.91	0.6648	1.04	0.3056	1.32	0.2009
NM_000636	*SOD2*	Superoxide dismutase 2, mitochondrial	1.41	**0.018**	1.17	0.4404	1.12	0.7714
Refseq	Symbol	Heat Shock						
NM_001539	*DNAJA1*	DnaJ (Hsp40) homolog, subfamily A, member 1	0.94	0.6648	1.00	0.9866	1.01	0.941
NM_007034	*DNAJB4*	DnaJ (Hsp40) homolog, subfamily B, member 4	1.20	0.2413	1.20	**0.034**	1.36	0.0958
NM_005526	*HSF1*	Heat shock transcription factor 1	0.84	0.3354	1.14	0.5016	1.22	0.505
NM_005345	*HSPA1A*	Heat shock 70 kDa protein 1A	1.11	0.6876	1.16	0.7269	1.44	0.6701
NM_005527	*HSPA1L*	Heat shock 70 kDa protein 1-like	0.92	0.5798	1.02	**0.0363**	1.71	0.2402
NM_021979	*HSPA2*	Heat shock 70 kDa protein 2	0.52	**0.0472**	0.91	0.8172	1.09	0.8536
NM_002154	*HSPA4*	Heat shock 70 kDa protein 4	0.93	0.742	1.04	0.9481	1.17	0.8293
NM_005347	*HSPA5*	Heat shock 70 kDa protein 5 (glucose-regulated protein, 78 kDa)	0.79	0.6034	1.14	0.6219	1.23	0.6163
NM_002155	*HSPA6*	Heat shock 70 kDa protein 6 (HSP70B')	3.17	**0.0441**	0.90	0.5741	2.82	0.2556
NM_006597	*HSPA8*	Heat shock 70 kDa protein 8	0.99	0.9686	1.01	0.9229	1.01	0.9507
NM_001540	*HSPB1*	Heat shock 27 kDa protein 1	0.78	0.2709	0.92	0.1562	1.26	0.6665
NM_001040141	*HSP90AA2*	Heat shock protein 90 kDa alpha (cytosolic), class A member 2	0.99	0.9698	0.75	0.0698	0.88	0.3659
NM_007355	*HSP90AB1*	Heat shock protein 90 kDa alpha (cytosolic), class B member 1	0.99	0.9456	1.01	0.8344	1.24	0.3531
NM_002156	*HSPD1*	Heat shock 60 kDa protein 1 (chaperonin 60)	1.11	0.3582	1.21	**0.0011**	1.46	0.4387
NM_002157	*HSPE1*	Heat shock 10 kDa protein 1 (chaperonin 10)	0.92	0.6773	1.14	0.2865	1.23	0.4716
NM_006644	*HSPH1*	Heat shock 105 kDa/110 kDa protein 1	0.90	0.4271	0.93	0.3818	0.92	0.4994
Refseq	Symbol	Proliferation and carcinogenesis						
NM_005190	*CCNC*	Cyclin C	0.81	0.4741	0.79	**0.0017**	1.14	0.7705
NM_053056	*CCND1*	Cyclin D1	1.80	**0.0463**	1.47	0.2166	1.05	0.8386
NM_004060	*CCNG1*	Cyclin G1	0.66	**0.013**	0.97	0.6882	1.12	0.5963
NM_005225	*E2F1*	E2F transcription factor 1	0.79	0.3984	0.88	0.6577	0.75	0.3307
NM_001964	*EGR1*	Early growth response 1	3.38	**0.0103**	2.49	**0.0282**	3.01	**0.0189**
NM_182649	*PCNA*	Proliferating cell nuclear antigen	0.74	**0.0451**	0.92	0.4305	0.92	0.7789

Refseq	Symbol	Growth arrest and senescence						
NM_000389	*CDKN1A*	Cyclin-dependent kinase inhibitor 1A (p21, Cip1)	1.31	**0.0469**	0.72	0.3465	0.82	0.161
NM_004083	*DDIT3*	DNA-damage-inducible transcript 3 (CHOP/GADD153)	1.54	0.2706	1.44	0.3976	2.62	**0.0001**
NM_001924	*GADD45A*	Growth arrest and DNA-damage-inducible, alpha	0.83	0.5737	0.55	**0.0097**	0.91	0.8843
NM_004864	*GDF15*	Growth differentiation factor 15	3.08	**0.0065**	1.14	0.055	1.54	**0.0065**
NM_002178	*IGFBP6*	Insulin-like growth factor binding protein 6	0.99	0.9655	1.31	**0.024**	1.72	0.4315
NM_002392	*MDM2*	Mdm2 p53 binding protein homolog (mouse)	1.19	**0.0275**	1.17	0.1598	1.67	0.3388
NM_000546	*TP53*	Tumor protein p53	1.39	0.5984	1.35	0.4127	1.39	0.1572
NM_002989	*CCL21*	Chemokine (C-C motif) ligand 21	1.53	0.3403	2.04	0.1551	1.39	0.1572
NM_002983	*CCL3*	Chemokine (C-C motif) ligand 3	1.05	0.9201	1.63	0.2926	0.86	0.583
NM_002984	*CCL4*	Chemokine (C-C motif) ligand 4	1.18	0.8063	1.27	0.6026	1.15	0.3721
NM_000758	*CSF2*	Colony stimulating factor 2 (granulocyte-macrophage)	2.18	0.3387	1.13	0.2069	1.22	0.6381
NM_001565	*CXCL10*	Chemokine (C-X-C motif) ligand 10	0.19	**0.0297**	0.40	0.111	0.16	**0.0068**
NM_001562	*IL18*	Interleukin 18 (interferon-gamma-inducing factor)	1.21	0.1195	0.54	0.112	0.50	0.1121
NM_000575	*IL1A*	Interleukin 1, alpha	0.73	0.0613	0.67	0.176	0.63	0.3962
NM_000576	*IL1B*	Interleukin 1, beta	0.80	0.2763	1.29	0.8008	0.87	0.3375
NM_000600	*IL6*	Interleukin 6 (interferon, beta 2)	0.85	0.6465	0.86	0.9153	0.81	0.8805
NM_000595	*LTA*	Lymphotoxin alpha (TNF superfamily, member 1)	1.33	0.5014	0.55	0.1135	1.20	0.7121
NM_002415	*MIF*	Macrophage migration inhibitory factor (glycosylation-inhibiting factor)	0.83	0.4905	0.92	0.5481	1.13	0.7
NM_003998	*NFKB1*	Nuclear factor of kappa light polypeptide gene enhancer in B-cells 1	2.41	0.2417	1.08	0.4045	1.09	0.6532
NM_000625	*NOS2*	Nitric oxide synthase 2, inducible	0.92	0.7952	1.92	0.5901	1.59	0.6917
NM_000602	*SERPINE1*	Serpin peptidase inhibitor (nexin, plasminogen activator inhibitor type 1), member 1	5.79	**0.0117**	1.67	**0.0023**	1.87	0.2379
Refseq	Symbol	Necrosis or apoptosis (DNA Damage and Repair)						
NM_000051	*ATM*	Ataxia telangiectasia mutated	1.00	0.9639	1.16	0.4761	1.51	**0.0443**
NM_007194	*CHEK2*	CHK2 checkpoint homolog (S. pombe)	0.89	0.6853	1.22	0.4784	1.29	0.601
NM_001923	*DDB1*	Damage-specific DNA binding protein 1, 127 kDa	0.85	0.3657	1.34	0.1644	1.49	0.265
NM_001983	*ERCC1*	Excision repair cross-complementing rodent repair deficiency, complementation group 1	1.04	0.7027	0.96	0.8973	1.29	0.4044
NM_000122	*ERCC3*	Excision repair cross-complementing rodent repair deficiency, complementation group 3 (xeroderma pigmentosum group B complementing)	0.82	0.5098	0.91	0.1597	0.93	**0.0111**
NM_005053	*RAD23A*	RAD23 homolog A (S. cerevisiae)	1.09	0.425	1.09	0.7593	1.51	0.3772
NM_005732	*RAD50*	RAD50 homolog (S. cerevisiae)	0.95	0.9025	1.15	0.7038	1.14	0.7021
NM_007120	*UGT1A4*	UDP glucuronosyltransferase 1 family, polypeptide A4	1.09	0.6556	0.44	0.0879	0.58	0.1384
NM_003362	*UNG*	Uracil-DNA glycosylase	0.93	0.5643	0.78	0.2949	1.08	0.8106
NM_006297	*XRCC1*	X-ray repair complementing defective repair in Chinese hamster cells 1	1.12	0.7654	0.69	0.2278	1.03	0.911
NM_005431	*XRCC2*	X-ray repair complementing defective repair in Chinese hamster cells 2	1.43	0.2942	0.92	0.2258	1.42	0.6878
Refseq	Symbol	Necrosis or apoptosis (apoptosis signaling)						
NM_001154	*ANXA5*	Annexin A5	1.18	0.0544	0.99	0.9696	1.42	0.1703
NM_004324	*BAX*	BCL2-associated X protein	0.81	0.2674	0.86	0.6249	1.27	0.6159
NM_138578	*BCL2L1*	BCL2-like 1	1.34	0.1308	0.96	0.4846	0.84	0.1026
NM_033292	*CASP1*	Caspase 1, apoptosis-related cysteine peptidase (interleukin 1, beta, convertase)	0.53	0.1466	0.72	0.5916	0.53	0.5695
NM_001230	*CASP10*	Caspase 10, apoptosis-related cysteine peptidase	0.85	0.5504	1.15	0.1948	1.52	0.3882
NM_001228	*CASP8*	Caspase 8, apoptosis-related cysteine peptidase	1.47	**0.0406**	1.88	0.0525	2.18	0.2462
NM_000639	*FASLG*	Fas ligand (TNF superfamily, member 6)	2.61	0.0895	0.91	0.8704	0.40	0.2122
NM_020529	*NFKBIA*	Nuclear factor of kappa light polypeptide gene enhancer in B-cells inhibitor, alpha	0.84	0.7175	0.76	0.0713	0.74	0.5306
NM_000594	*TNF*	Tumor necrosis factor (TNF superfamily, member 2)	1.80	**0.0287**	0.47	**0.0053**	0.47	**0.0128**
NM_001065	*TNFRSF1A*	Tumor necrosis factor receptor superfamily, member 1A	1.18	0.6517	1.13	0.2754	1.29	0.4533
NM_003810	*TNFSF10*	Tumor necrosis factor (ligand) superfamily, member 10	0.16	**0.0016**	0.69	0.19	0.70	0.518
Refseq	Symbol	House-keeping						
NM_004048	*B2M*	Beta-2-microglobulin						
NM_000194	*HPRT1*	Hypoxanthine phosphoribosyltransferase 1						
NM_012423	*RPL13A*	Ribosomal protein L13a						
NM_002046	*GAPDH*	Glyceraldehyde-3-phosphate dehydrogenase						
NM_001101	*ACTB*	Actin, beta						

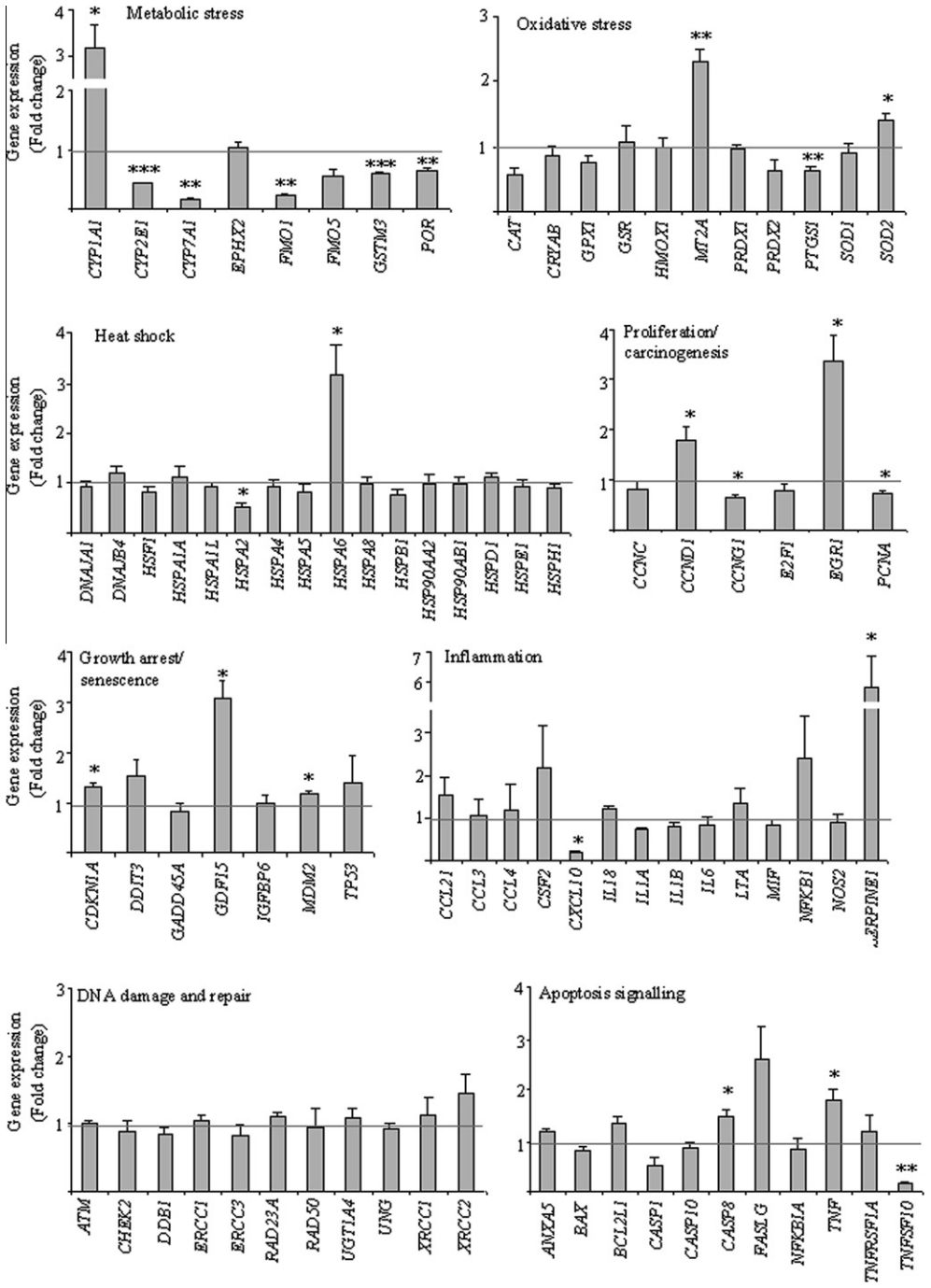

Fig. 1. Differential expression of 6 groups of stress and toxicity response-related genes in Hep3B cells treated with 10 μM EFV for 8 h. The expression of each gene was normalized to the mean of the mRNA level of the house-keeping genes. Data (mean ± SEM, $n = 3$), are represented as fold change of expression with respect to that recorded in the vehicle-treated cells, which was considered 1. Statistical analysis: Student's t-test, $^{*}p < 0.05$, $^{**}p < 0.01$, $^{***}p < 0.001$ vs vehicle.

dase inhibitor, clade E (*SERPINE1*), whereas Chemokine (C-X-C motif) ligand 10 (*CXCL10*) displayed decreased mRNA levels. Several Chemokine (C-C motif) ligands and interleukins, as well as colony stimulating factor 2 (*CSF2*), Nitric oxide synthase 2 (*NOS2*), Lymphotoxin alpha (*LTA*) and Macrophage migration inhibitory factor (*MIF*), were also evaluated but showed no changes. Among the 22 genes related to necrosis and apoptosis, only Caspase 8 (*CASP8*) and Tumor necrosis factor (*TNF*) were significantly up-regulated. BCL2-like 1 (*BCL2L1*) and Fas ligand (*FASLG*) also manifested increases, albeit without statistical significance, whereas Tumor necrosis factor (ligand) superfamily member 10 (*TNFSF10*) was down-regulated.

When gene expression was analyzed following a longer period of exposure (24 h) to EFV (10 and 25 μM), most of the results were in line with the trend observed following 8 h-treatment. Regarding metabolic stress, both EFV concentrations led to a significant increase in the expression of *CYP1A1*, whereas that of *FMO1* remained down-regulated. *CYP2E1*, *CYP7A1*, *POR* and *GSTM3* displayed mRNA levels similar to those detected in vehicle-treated cells, with the exception of Epoxide hydrolase 2 (*EPHX2*), which was up-regulated by EFV 25 μM. Among the oxidative stress-responsive genes, only *MT2A* continued to be up-regulated in a concentration related manner, whereas *CRYAB* and *PTGS1* were down-regulated. Interestingly, neither *CAT* nor *SOD2* showed changes. Among the HSP,

expression of *HSPA6* was up-regulated in cells treated with EFV 25 μM, but not in those incubated with 10 μM. Of the genes implicated in proliferation and/or carcinogenesis, only *EGR1* remained significantly up-regulated, and in a concentration-dependent manner. Of the genes associated with growth arrest and senescence, *GDF15* remained highly up regulated in a concentration-dependent manner, and a similar trend towards an increase was detected with *MDM2*, *IGFBP6* and *TP53*. Significantly, at this point we detected a major increase in *DDIT3* mRNA levels, particularly after treatment with 25 μM EFV. The profile observed in the expression of the genes related to inflammation did not differ significantly between 8 and 24 h of EFV treatment; in fact, the only variation observed was a diminished mRNA content among several interleukins. Of the genes associated with necrosis or apoptosis, only *CASP8* continued to show the increase exhibited after 8 h exposure to EFV, though this increment was now found to be concentration-dependent, whereas a non-significant decrease was observed for *CASP1* and *TNFSF10*. In the case of *ATM* mRNA, a significant increase was detected. Intriguingly, *FASLG* and *TNF* were seen to be down-regulated, despite showing an enhanced expression following 8 h treatment.

In addition, we validated the expression of several functionally important genes which manifested differential expression in the array, by performing individual real-time RT-PCR at 8 h and 24 h treatment with 10 and 25 μM EFV. In accordance with the results obtained from the gene array, *ATM*, *EGR1*, *HSPA6*, *MT2A* and *SERPINE1* displayed up-regulation which occurred in a concentration-dependent manner (except for *SERPINE1*), and reached statistical significance in *EGR1*, *MT2A* and *SERPINE1*, as shown in Fig. 2. As expected, the expression of *CXCL10* was diminished.

Taking into consideration the published evidence of EFV-induced oxidative stress and mitochondrial damage in hepatic cells, we found particularly interesting the increase in the expression of *HSPA6* and *MT2A*. In order to further confirm this result we performed western blot analysis using whole-cell protein extracts which showed significantly enhanced protein levels of both HSAP6 and MT2A after 24 h treatment with 10 and 25 μM EFV (Fig. 3).

In order to rule out that the observed effects were related to the hepatocellular carcinoma cell line chosen for this study (Hep3B), we performed several confirmatory experiments using primary human hepatocytes. As shown in Fig. 4A, *ATM*, *EGR1*, *HSPA6*, *MT2A* and *SERPINE1* displayed up-regulated expression after treatment with EFV (10 and 25 μM) for 24 h. On the contrary, the level of *CXCL10* mRNA did not change significantly and only displayed a slight tendency of decrease. Also, in line with the results obtained in Hep3B, both HSPA6 and MT2A showed enhanced protein expression in EFV-treated primary hepatic cells (Fig. 4B).

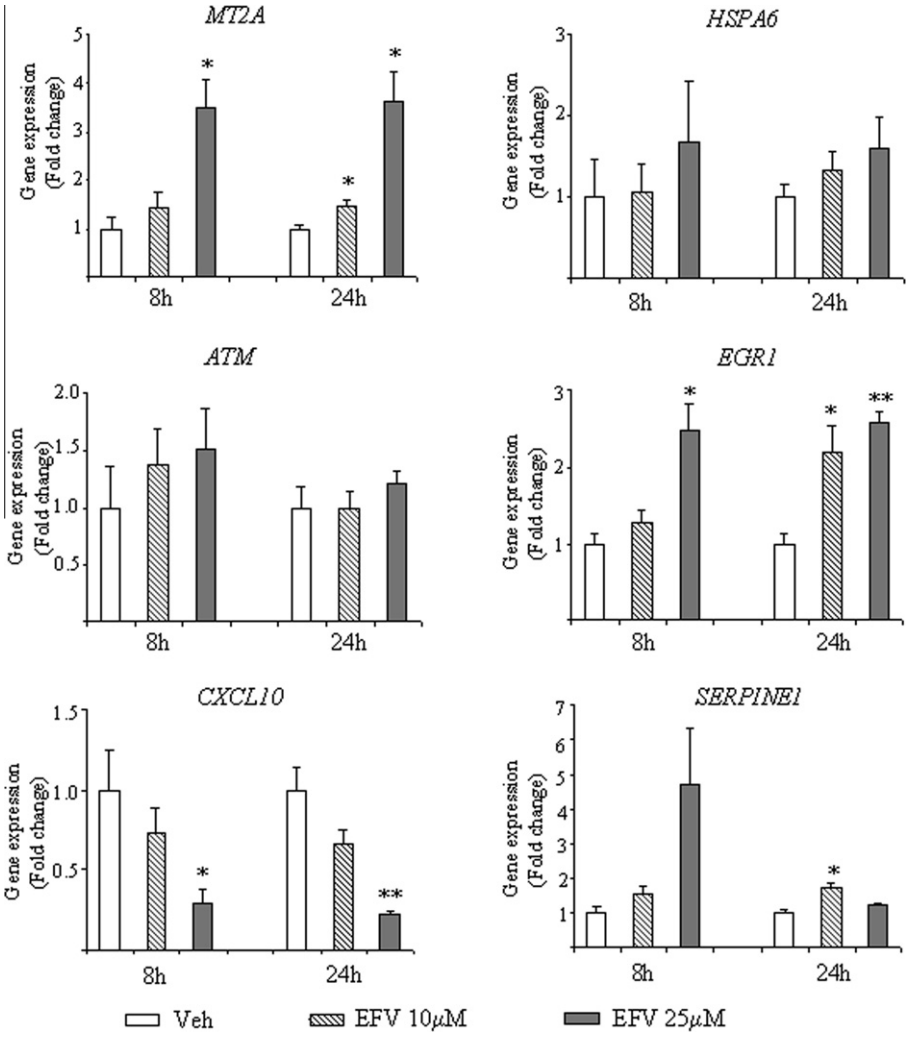

Fig. 2. Individual real-time RT-PCR of selected genes after treatment of Hep3B cells with 10 μM or 25 μM EFV for 8 h and 24 h. Expression levels were normalized to the expression of Cyclophilin A, which was employed as a house-keeping gene. Data (mean ± SEM, $n = 3$-4), are represented as fold change of expression with respect to that recorded in the vehicle-treated cells, which was considered 1. Statistical analysis: Student's t-test, $^{*}p < 0.05$, $^{**}p < 0.01$, vs vehicle.

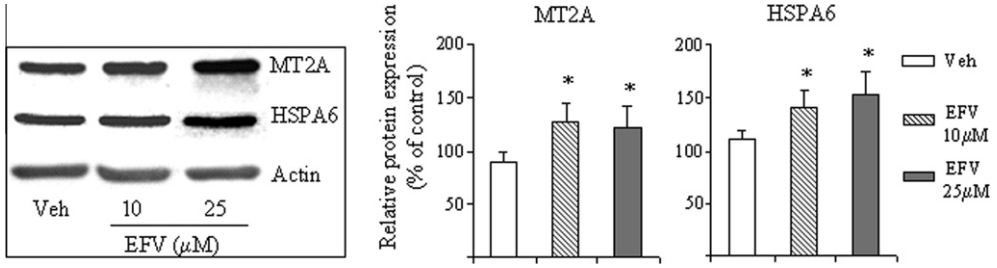

Fig. 3. Western blot analysis of the expression of HSPA6 and MT2A after treatment of Hep3B cells with 10 μM or 25 μM EFV for 24 h. Representative images are provided and a summary of densitometry data (mean ± SEM, $n = 6–7$) expressed as protein expression in relation to that of untreated cells in each individual experiment, which was considered 100%, $^{*}p < 0.05$ vs vehicle.

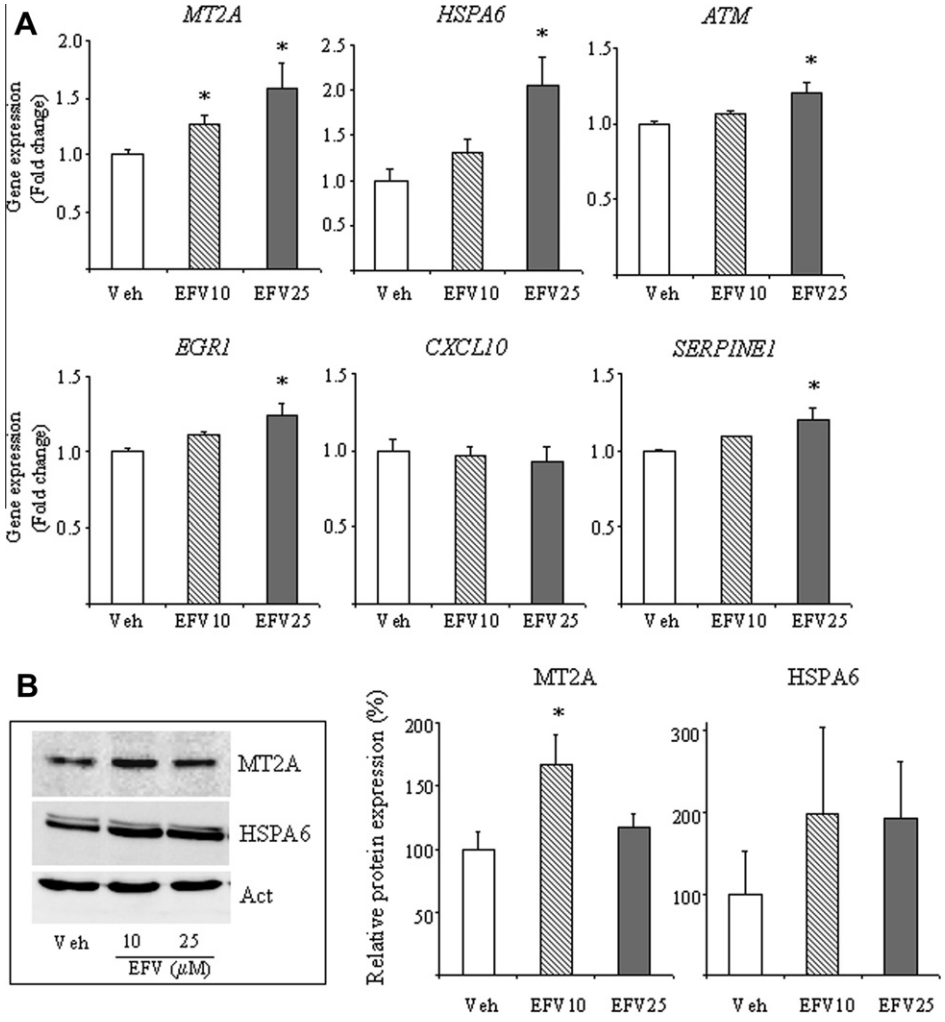

Fig. 4. Expression profiles of selected genes in primary human hepatocytes after treatment with 10 μM or 25 μM EFV for 24 h. A. Individual real-time RT-PCR of selected genes whose expression levels were normalized to the expression of Cyclophilin A, which was employed as a house-keeping gene. Data (mean ± SEM, $n = 3$), are represented as fold change of expression with respect to that recorded in the vehicle-treated cells, which was considered 1. B. Western blot analysis of the expression of HSPA6 and MT2A. Representative images are shown and a summary of densitometry data (mean ± SEM, $n = 3$) expressed as protein expression in relation to that of vehicle-treated cells (considered 100%). Statistical analysis: Student's t-test, $^{*}p < 0.05$, vs vehicle.

4. Discussion

Recent studies in human hepatic cells have described that EFV elicits stress-related responses involving mitochondrial dysfunction and oxidative stress, the consequences of which may play a role in some side effects attributed to this drug (Apostolova et al., 2010; Blas-García et al., 2010; Apostolova et al., 2011). To expand these findings, we have analyzed the influence of EFV on the expression profile of relevant stress- and toxicity-genes in Hep3B cells. Modified mRNA levels are a good marker of a "trend" in gene expression, particularly when considering groups of selected genes involved in specific functions, although it is important to point out that such a "trend" may not always correlate well with protein expression or function. As a general overview, our results reveal substantial modifications in several of the early response-, oxidative stress- and damage-related genes which are clearly supportive

of previously published findings of altered mitochondrial function and increases in ROS after treatment with EFV. We detected an increased expression of *MT2A*, a member of the Metallothionein family, small stress-induced cysteine-rich proteins (6–7 kDa) whose induction is considered an adaptive mechanism that directly correlates with the magnitude and progression of toxicological injury in the liver (Kurowska and Bal, 2010). Metallothioneins participate in ion homeostasis by binding with metals and in the prevention of oxidative stress by scavenging ROS in a way that resembles glutathione (Thornalley and Vasák, 1985). *MT2A* expression increases upon induction of oxidative stress in cellular models, such as human lymphoma cells exposed to the antineoplastic agent gallium nitrate (Yang and Chitambar, 2008) or in HeLa cells treated with rotenone, an inhibitor of mitochondrial complex I (Reinecke et al., 2006). The latter finding is relevant to our previous report in which EFV–treated hepatic cells exhibited decreased respiration attributed to a defect of mitochondrial Complex I, an effect which was accompanied by increased ROS (Blas-García et al., 2010). Importantly MT2A-overexpression is positively related to maintenance of cellular ATP levels, $\Delta\Psi_m$ and cell viability in HeLa cells treated with rotenone (Reinecke et al., 2006). In addition, we detected a slight decrease in the expression of other oxidative-stress genes, such as *PTGS1*. Although somewhat paradoxical, such a reduction has previously been reported as being part of specific cell responses to redox challenges and being related to the duration of the stress-stimuli or feed-back mechanisms. For example, a 6-fold decrease in *PTGS1* mRNA has been reported in IMR-90 human embryo fibroblasts following 6 days of mild oxidative stress (Faraonio et al., 2002).

In relation with stress- and protein damage-responsive genes, EFV treatment leads to up-regulation of *HSPA6*, an Hsp70 chaperone unique to primates. Accumulation of proteasome substrates and proteotoxic conditions are potent inducers of this strictly stress-inducible gene, and it has been postulated that Hsp70B′, the protein product of *HSPA6*, aids resistance to cell death in pathological conditions of increased accumulation of damaged proteins. However, since *HSPA6* up-regulation is only transient, high levels of this protein may be detrimental if maintained (Noonan et al., 2007). Furthermore, *HSPA6* is an unusual HSP, as it does not contain the generic chaperone-like properties of other HSP70s and may have evolved to maintain specific critical functions under conditions of severe stress (Hageman et al., 2011).

Our results also reveal a certain increase in *ATM*, a gene related to DNA damage and which encodes a multifunctional serine/threonine kinase whose activity is augmented by DNA-double strand breaks. ATM participates in oxidative defence by up-regulating major antioxidants, including superoxide dismutase, catalase, glutathione peroxidase, and glutathione reductase (Barzilai et al., 2002). Furthermore, *Atm*-deficiency has been related to specific oxidative stress responses such as endoplasmatic reticulum (ER) stress and unfolded protein response (UPR) (Yan et al., 2008).

Similarly, we have observed alterations in the expression of various genes involved in proliferation and growth arrest/senescence. In particular, there was a substantial increase in *GDF15*, a member of the transforming growth factor beta (TGF-β) superfamily implicated in tissue homeostasis, differentiation, remodelling and repair through the regulation of inflammatory and apoptotic pathways. Specifically, *GDF15* up-regulation has been reported during pathological conditions such as tissue hypoxia, oxidative stress and injury (Zimmers et al., 2006), and has been linked to the prevention of apoptosis and reduction of ROS levels (Subramaniam et al., 2003). *DDIT3* encodes a member of the CCAAT/enhancer binding protein(C/EBP) family of transcription factors (largely known as CHOP/GADD153). Besides its role in ER stress, it is transcriptionally induced in response to mitochondria-related oxidative stress and forms part of the mitochondrial UPR signalling pathway through the trans-regulation of several mitochondrial chaperones and proteases (Haynes and Ron, 2010). The mitochondrial UPR response is triggered by the accumulation of unfolded or misfolded proteins in the mitochondrial matrix, which occurs as a result of (a) the dysfunction of this organelle; (b) an increased mitochondrial biogenesis and protein import; or (c) the presence of damaging agents such as ROS. We also report an increase of the transcription regulator EGR-1, a member of the immediate-early gene family that acts as a tumor suppressor and is involved in cell growth and differentiation in response to a long list of signals, including stress. EGR1 was found to be up-regulated in a scenario similar to that presented here, involving platycodin D-induced mitochondrial dysfunction and enhanced generation of ROS in U937 cells. In the study in question, ROS-dependent EGR-1 activation was considered essential for the regulation of apoptosis induced by platycodin D, a natural triterpenoid saponin with anti-inflammatory properties (Shin et al., 2009). In addition, a similar profile of changes in gene expression associated with genotoxic stress responses and DNA repair or cell cycle progression has recently been described in alveolar epithelial A549 cells with another typically prooxidant molecule, paraquat, and postulated to contribute to the cytotoxicity of this compound (Mitsopoulos and Suntres, 2010).

Regarding metabolic stress, we observed increased expression of cytochrome P450 *CYP1A1*, one of the three members of the CYP1 family. This enzyme participates in the metabolism of xenobiotics and some endogenous substrates, and is transcriptionally activated by many exogenous ligands, notably drugs and environmental pollutants. The function of CYP1A1 appears to be much more complex than was initially believed, as it seems to play more than a toxicological role. For instance, recent investigations suggest that it functions as a carcinogen-detoxication enzyme, whereas its involvement in the activation of natural dietary compounds with chemopreventative activity points to a cancer-protective role (Androutsopoulos et al., 2009). Unlike other members of the same family, CYP1A1 is not only found in ER and depending on the tissue or inducer in question, it can be located in the mitochondrial inner membrane as reported for rat liver pretreated with β-napthoflavone. Interestingly, mtCYP1A1 displays distinct substrate specificity related to the presence of other coenzymes in this compartment (Androutsopoulos et al., 2009).

We also report significant variations in the expression of two inflammation-related genes; the cytokine *SERPINE1* displayed elevated mRNA levels whereas the chemokine *CXCL10* (also called IP-10) was found to be diminished after treatment with EFV. Up-regulation of SERPINE1 (also called PAI-1) has been associated with the liver damage present in alcoholic liver disease, haemorrhagic shock, bile duct ligation and acetaminophen hepatotoxicity (Dimova and Kietzmann, 2008). The decrease observed in CXCL10 levels is intriguing, since an increased expression of this gene has been associated with liver injury, including hepatitis infection. However, the reduction of its levels through the use of pharmacological agents has been shown to be protective in models of ischemia and reperfusion liver injury (Tsuchihashi et al., 2006; Shen et al., 2007).

Importantly, the gene array was validated by individual RT-PCRs of six representative genes; the expression of two of them was also assessed at the protein level.

Moreover, we confirmed these results using primary human hepatocytes giving greater physiological relevance to the findings described in Hep3B cells. The exception was the level of *CXCL10* mRNA which unlike the rest of the analyzed genes whose changes followed the pattern observed in Hep3B cells, only displayed a slight tendency of decrease. The discrepancy may be due to the time-frame employed in this experiment (24 h) and it is possible that the observed effect in primary hepatic cells may become more pronounced if the treatment period is prolonged.

To our knowledge, the present work in is the first to report significant variations in the expression of a panel of genes related to toxicity and stress responses in EFV-treated cells. These changes may be relevant for the understanding of the hepatic adverse events associated to the clinical use of EFV. Importantly, Nevirapine (NVP), the other NNRTI commonly applied in cART, is also considered to have potential for hepatotoxicity. However, previous studies by our group have shown that this drug does not induce any of the mitochondrial (compromised mitochondrial respiration, diminished $\Delta\Psi_{m,}$ increased ROS generation) and metabolic alterations (decreased ATP level and increased intracellular accumulation of lipids) that were detected in Hep3B cells treated with EFV (Blas-García et al., 2010). Therefore, EFV and NVP may display very different molecular profiles of liver damage, presumably due to the distinct chemical properties of the two drugs. The genes we found to be affected by EFV are implicated in drug metabolism and are related to modifications in the cellular redox status/oxidative stress, which is in keeping with previously published data demonstrating altered mitochondrial function and increased ROS levels in EFV-treated hepatic cells. The results obtained regarding genes involved in inflammation, carcinogenesis or apoptosis signaling need to be further supported and additional studies will permit the consideration of these findings in a more specific cellular context.

Acknowledgements

The authors thank Brian Normanly for his English language editing.

This work was financed by the Grants PI11/00327 (Proyectos de Investigación en Salud, Ministerio de Ciencia e Innovación), CIBER CD06/04/0071 (Ministerio de Sanidad y Consumo), PROMETEO/2010/060 and ACOMP/2010/207 (both from the Generalitat Valenciana). N.A. is a recipient of a Juan de la Cierva contract (JCI-2011-11357, Ministerio de Ciencia e Innovación).

References

AIDSinfo (2011). A service of the U.S. Department of Health and Human Services. Guidelines for the use of antiretroviral agents in HIV-1-infected adults and adolescents. <http://aidsinfo.nih.gov/Guidelines/Default.aspx?MenuItem=Guidelines> (accessed 15.02.12).

Androutsopoulos, V.P., Tsatsakis, A.M., Spandidos, D.A., 2009. Cytochrome P450 CYP1A1: wider roles in cancer progression and prevention. BMC Cancer 9, 187.

Apostolova, N., Gomez-Sucerquia, L.J., Moran, A., Alvarez, A., Blas-Garcia, A., Esplugues, J.V., 2010. Enhanced oxidative stress and increased mitochondrial mass during efavirenz-induced apoptosis in human hepatic cells. Br. J. Pharmacol. 160 (8), 2069–2284.

Apostolova, N., Gomez-Sucerquia, L.J., Gortat, A., Blas-Garcia, A., Esplugues, J.V., 2011. Compromising mitochondrial function with the antiretroviral drug efavirenz induces cell survival-promoting autophagy. Hepatology 54 (3), 1009–1019.

Barzilai, A., Rotman, G., Shiloh, Y., 2002. ATM deficiency and oxidative stress: a new dimension of defective response to DNA damage. DNA Repair (Amst) 1 (1), 3–25.

Blas-García, A., Apostolova, N., Ballesteros, D., Monleón, D., Morales, J.M., Rocha, M., Victor, V.M., Esplugues, J.V., 2010. Inhibition of mitochondrial function by efavirenz increases lipid content in hepatic cells. Hepatology 52 (1), 115–125.

Burger, D., van der Heiden, I., la Porte, C., van der Ende, M., Groeneveld, P., Richter, C., Koopmans, P., Kroon, F., Sprenger, H., Lindemans, J., Schenk, P., van Schaik, R., 2006. Interpatient variability in the pharmacokinetics of the HIV non-nucleoside reverse transcriptase inhibitor efavirenz: the effect of gender, race, and *CYP2B6* polymorphism. Br. J. Clin. Pharmacol. 61 (2), 148–154.

Caron-Debarle, M., Lagathu, C., Boccara, F., Vigouroux, C., Capeau, J., 2010. HIV-associated lipodystrophy: from fat injury to premature aging. Trends Mol. Med. 16 (5), 218–229.

Dimova, E.Y., Kietzmann, T., 2008. Metabolic, hormonal and environmental regulation of plasminogen activator inhibitor-1 (PAI-1) expression: lessons from the liver. Thromb. Haemost. 100 (6), 992–1006.

Faraonio, R., Pane, F., Intrieri, M., Russo, T., Cimino, F., 2002. In vitro acquired cellular senescence and aging-specific phenotype can be distinguished on the basis of specific mRNA expression. Cell Death Differ. 9 (8), 862–864.

Gutierrez, F., Navarro, A., Padilla, S., Anton, R., Masia, M., Borras, J., Martín-Hidalgo, A., 2005. Prediction of neuropsychiatric adverse events associated with long-term efavirenz therapy, using plasma drug level monitoring. Clin. Infect. Dis. 41 (11), 1648–1653.

Hageman, J., van Waarde, M.A., Zylicz, A., Walerych, D., Kampinga, H.H., 2011. The diverse members of the mammalian HSP70 machine show distinct chaperone-like activities. Biochem. J. 435 (1), 127–142.

Haynes, C.M., Ron, D., 2010. The mitochondrial UPR – protecting organelle protein homeostasis. J. Cell Sci. 123 (Pt 22), 3849–3855.

Inductivo-Yu, I., Bonacini, M., 2008. Highly active antiretroviral therapy-induced liver injury. Curr. Drug Saf. 3 (1), 4–13.

Kurowska, E., Bal, W., 2010. Recent advances in molecular toxicology of cadmium and nickel. In: Advances in Molecular Toxicology. pp. 85-126.

Lin, J., Schyschka, L., Mühl-Benninghaus, R., Neumann, J., Hao, L., Nussler, N., Dooley, S., Liu, L., Stöckle, U., Nussler, A.K., Ehnert, S., 2012. Comparative analysis of phase I and II enzyme activities in 5 hepatic cell lines identifies Huh-7 and HCC-T cells with the highest potential to study drug metabolism. Arch. Toxicol. 86 (1), 87–95.

Maggiolo, F., 2009. Efavirenz: a decade of clinical experience in the treatment of HIV. J. Antimicrob. Chemother. 64 (5), 910–928.

Manfredi, R., Calza, L., Chiodo, F., 2005. An extremely different dysmetabolic profile between the two available nonnucleoside reverse transcriptase inhibitors: efavirenz and nevirapine. J. Acq. Immun. Def. Synd. 38 (2), 228–236.

Mitsopoulos, P., Suntres, Z.E., 2010. Cytotoxicity and gene array analysis of alveolar epithelial A549 cells exposed to paraquat. Chem. Biol. Interact. 188 (3), 427–436.

Noonan, E.J., Place, R.F., Giardina, C., Hightower, L.E., 2007. Hsp70B' regulation and function. Cell Stress Chaperon. 12 (4), 393–402.

Núñez, M., 2006. Hepatotoxicity of antiretrovirals: incidence, mechanisms and management. J. Hepatol. 44 (1 Suppl), S132–S139.

Núñez, M., 2010. Clinical syndromes and consequences of antiretroviral-related hepatotoxicity. Hepatology 52 (3), 1143–1155.

Reinecke, F., Levanets, O., Olivier, Y., Louw, R., Semete, B., Grobler, A., Hidalgo, J., Smeitink, J., Olckers, A., Van der Westhuizen, F.H., 2006. Metallothionein isoform 2A expression is inducible and protects against ROS-mediated cell death in rotenone-treated HeLa cells. Biochem. J. 395 (2), 405–415.

Shen, X.D., Ke, B., Zhai, Y., Tsuchihashi, S.I., Gao, F., Duarte, S., Coito, A., Busuttil, R.W., Allison, A.C., Kupiec-Weglinski, J.W., 2007. Diannexin, a novel annexin V homodimer, protects rat liver transplants against cold ischemia-reperfusion injury. Am. J. Transplant. 7 (11), 2463–2471.

Shin, D.Y., Kim, G.Y., Li, W., Choi, B.T., Kim, N.D., Kang, H.S., Choi, Y.H., 2009. Implication of intracellular ROS formation, caspase-3 activation and Egr-1 induction in platycodon D-induced apoptosis of U937 human leukemia cells. Biomed. Pharmacother. 63 (2), 86–94.

Subramaniam, S., Strelau, J., Unsicker, K., 2003. Growth differentiation factor-15 prevents low potassium-induced cell death of cerebellar granule neurons by differential regulation of Akt and ERK pathways. J. Biol. Chem. 278 (11), 8904–8912.

Tashima, K.T., Bausserman, L., Alt, E.N., Aznar, E., Flanigan, T.P., 2003. Lipid changes in patients initiating efavirenz- and indinavir-based antiretroviral regimens. HIV Clin. Trials 4 (1), 29–36.

Thornalley, P.J., Vasák, M., 1985. Possible role for metallothionein in protection against radiation-induced oxidative stress. Kinetics and mechanism of its reaction with superoxide and hydroxyl radicals. Biochim. Biophys. Acta 827 (1), 36–44.

Tsuchihashi, S., Kaldas, F., Chida, N., Sudo, Y., Tamura, K., Zhai, Y., Qiao, B., Busuttil, R.W., Kupiec-Weglinski, J.W., 2006. FK330, a novel inducible nitric oxide synthase inhibitor, prevents ischemia and reperfusion injury in rat liver transplantation. Am. J. Transplant. 6 (9), 2013–2022.

Walker, U.A., Setzer, B., Venhoff, N., 2002. Increased long-term mitochondrial toxicity in combinations of nucleoside analogue reverse-transcriptase inhibitors. AIDS 16, 2165–2173.

Yan, M., Shen, J., Person, M.D., Kuang, X., Lynn, W.S., Atlas, D., Wong, P.K., 2008. Endoplasmic reticulum stress and unfolded protein response in Atm-deficient thymocytes and thymic lymphoma cells are attributable to oxidative stress. Neoplasia 10 (2), 160–167.

Yang, M., Chitambar, C.R., 2008. Role of oxidative stress in the induction of metallothionein-2A and heme oxygenase-1 gene expression by the antineoplastic agent gallium nitrate in human lymphoma cells. Free Radic. Biol. Med. 45 (6), 763–772.

Zhu, X.H., Wang, C.H., Tong, Y.W., 2007. Growing tissue-like constructs with Hep3B/HepG2 liver cells on PHBV microspheres of different sizes. J. Biomed. Mater. Res. B. Appl. Biomater. 82 (1), 7–16.

Zimmers, T.A., Jin, X., Hsiao, E.C., Perez, E.A., Pierce, R.H., Chavin, K.D., Koniaris, L.G., 2006. Growth differentiation factor-15: induction in liver injury through p53 and tumor necrosis factor-independent mechanisms. J. Surg. Res. 130 (1), 45–51.